© 2016. Published by The Company of Biologists Ltd | Journal of Cell Science (2016) 129, 29-38 doi:10.1242/jcs.176412

RESEARCH ARTICLE

N-linked glycosylation plays a crucial role in the secretion of HMGB1

Young Hun Kim[1,2,*], Man Sup Kwak[1,*], Jun Bae Park[3], Shin-Ae Lee[1], Ji Eun Choi[4], Hyun-Soo Cho[3,‡] and Jeon-Soo Shin[1,2,5,‡]

ABSTRACT

HMGB1 protein is a delayed mediator of sepsis that is secreted to the extracellular milieu in response to various stimulants, inducing a pro-inflammatory response. HMGB1 is devoid of an endoplasmic reticulum (ER)-targeting signal peptide; hence, the mechanism of extracellular secretion is not completely understood, although HMGB1 is secreted after being subjected to post-translational modifications. Here, we identified the role of N-glycosylation of HMGB1 in extracellular secretion. We found two consensus (N37 and N134) and one non-consensus (N135) residues that were N-glycosylated in HMGB1 by performing liquid chromatography tandem mass spectrometry (LC-MS/MS) and analyzing for N-glycan composition and structure. Inhibition of N-glycosylation with tunicamycin resulted in a molecular shift of HMGB1 as assessed by gel electrophoresis. Non-glycosylated double mutant (N→Q) HMGB1 proteins ($HMGB1^{N37Q/N134Q}$ and $HMGB1^{N37Q/N135Q}$) showed localization to the nuclei, strong binding to DNA, weak binding to the nuclear export protein CRM1 and rapid degradation by ubiquitylation. These mutant proteins had reduced secretion even after acetylation, phosphorylation, oxidation and exposure to pro-inflammatory stimuli. Taken together, we propose that HMGB1 is N-glycosylated, and that this is important for its DNA interaction and is a prerequisite for its nucleocytoplasmic transport and extracellular secretion.

KEY WORDS: HMGB1, N-glycosylation, Post-translational modification, DNA binding, Secretion

INTRODUCTION

High mobility group box 1 (HMGB1) is a damage-associated molecular pattern (DAMP) molecule located in the nucleus. HMGB1 is secreted from activated monocytes and macrophages after post-translational modification (PTM) (Bonaldi et al., 2003; Youn and Shin, 2006), activation of an inflammasome pathway mediated by double-stranded RNA-dependent protein kinase (PKR, also known as EIF2AK2) (Lu et al., 2012), and through a pyruvate kinase M2 (PKM)-mediated pathway (Yang et al., 2014). HMGB1 is secreted through a non-classical vesicle-mediated secretory pathway (Gardella et al., 2002; Dupont et al., 2011). Additionally, HMGB1 can be released from dying cells as a result of autophagy (Thorburn et al., 2009), apoptosis (Bell et al., 2006), pyroptosis (Nyström et al., 2013) and necroptosis (programmed necrosis) mechanisms (Zou et al., 2013). HMGB1 can also initiate inflammation (Scaffidi et al., 2002), and it has a role as a late mediator of sepsis in both animal models and human patients (Ombrellino et al., 1999; Wang et al., 1999; Sundén-Cullberg et al., 2005). Extracellular HMGB1 binds to toll-like receptor (TLR) 2 and 4, as well as the receptor for advanced glycation end products (RAGE), and activates NF-κB and extracellular-signal-regulated protein kinases 1 and 2 (ERK1/2, also known as MAPK3 and MAPK1, respectively) (Salmivirta et al., 1992; Hori et al., 1995; Park et al., 2004) during sterile inflammation (Yang et al., 2010, 2015). HMGB1 interacts with host molecules of interleukin (IL)-1β (Sha et al., 2008), chemokine (C-X-C motif) ligand 12 (CXCL12) (Schiraldi et al., 2012) and nucleosomes (Tian et al., 2007), as well as with pathogen-associated molecular pattern (PAMP) molecules of lipopolysaccharide (LPS) and lipoteichoic acid (LTA), which are finally transferred to TLR4 and TLR2 receptors, respectively (Youn et al., 2008; Kwak et al., 2015), and augment or modify pro-inflammatory reactions. Intracellular HMGB1 is primarily located in the nucleus, where it functions as a nucleosome stabilizer and a regulator of transcription (Einck and Bustin, 1985; Lotze and Tracey, 2005), and also as a chaperone-like molecule that inhibits aggregation of polyglutamine (Min et al., 2013). In addition, HMGB1 binds to beclin-1 and regulates induction of autophagy (Tang et al., 2010).

Approximately 30 years ago, HMGB1 was reported to undergo extensive PTMs, including acetylation (Sterner et al., 1979; Dimov et al., 1990), phosphorylation (Sun et al., 1980; Kimura et al., 1985), methylation (Boffa et al., 1979) and adenosine diphosphate (ADP)-ribosylation (Tanuma et al., 1985). More recently, the molecular aspects of HMGB1 PTMs [acetylation (Bonaldi et al., 2003), phosphorylation (Youn and Shin, 2006), methylation (Ito et al., 2007), and cysteine oxidation (Hoppe et al., 2006)] have been investigated to determine the regulation of intracellular localization and extracellular secretion of HMGB1 owing to its role as an inflammatory mediator. The shuttling of HMGB1 between the nucleus and the cytoplasm is tightly regulated; the nuclear importin protein karyopherin-α1 and the nuclear exportin chromosomal maintenance 1 (CRM1, also known as XPO1) are involved in nucleocytoplasmic shuttling, which is influenced by modifications of HMGB1 (Bonaldi et al., 2003; Youn and Shin, 2006). HMGB1 has no signal peptide targeting it to the endoplasmic reticulum (ER), but a low degree of glycosyl modification has been identified in HMGB1 in calf thymus (Reeves and Chang, 1983; Elton and Reeves, 1986). The glycosylation residue and its role, however, have not been identified at a molecular level, although glycosylation is an important PTM.

[1]Department of Microbiology, Yonsei University College of Medicine, Seoul 120-752, Korea. [2]Brain Korea 21 PLUS Project for Medical Science, Yonsei University College of Medicine, Seoul 120-752, Korea. [3]Department of Systems Biology, Yonsei University College of Life Science and Biotechnology, Seoul 120-749, Korea. [4]Department of Pediatrics, Seoul National University Boramae Hospital, Seoul National University College of Medicine, Seoul 156-707, Korea. [5]Severance Biomedical Science Institute and Institute for Immunology and Immunological Diseases, Yonsei University College of Medicine, Seoul 120-752, Korea.
*These authors contributed equally to this work

‡Authors for correspondence (hscho8@yonsei.ac.kr; jsshin6203@yuhs.ac)

Received 25 June 2015; Accepted 9 November 2015

Journal of Cell Science (2016) 129, 29-38 doi:10.1242/jcs.176412

HMGB1 has two N-glycosylation acceptor sites with a consensus motif of NxS/T (x can be any amino acid other than proline) (Welply et al., 1983 Marshall, 1974; Gavel and von Heijne, 1990). Here, we demonstrated that HMGB1 can be N-glycosylated at the consensus motifs at N37 and N134, and at a non-consensus motif at N135, by using liquid chromatography tandem mass spectrometry (LC-MS/MS) and gel shift analysis of the double mutant HMGB1$^{N37Q/N134Q}$. De-glycosylation of HMGB1 increases its binding to DNA and decreases its binding to CRM1, as demonstrated through gel shift and fluorescence recovery after photobleaching (FRAP) assays. We found that de-glycosylated HMGB1 localized to the nucleus and showed little extracellular secretion even when it had other PTMs. These results demonstrate, at a molecular level, that HMGB1 can be glycosylated at three asparagine residues, and that this modification is an important prerequisite for cytoplasmic transport and extracellular secretion resulting from pro-inflammatory stimuli.

RESULTS

HMGB1 is N-glycosylated

The PTMs of HMGB1 are important for HMGB1 nucleocytoplasmic shuttling, extracellular secretion and transcriptional regulation. However, HMGB1 glycosylation and the functional role of this glycosylation have not been well characterized. The motif for N-linked glycosylation is NxS/T and there are four asparagine residues in HMGB1. Two motifs located at N37 and N134, in the HMGB1 A and B box, respectively, are part of this NxS/T motif. These motifs are conserved in rhesus macaques, cattle, rats, mice and chickens according to an N-linked glycosylation prediction program (NetNglyc, http://www.cbs.dtu.dk/services/NetNGlyc/) (Fig. 1A). Wild-type human HMGB1 (HMGB1^{WT}) does not contain an ER-targeting signal peptide to allow for glycosylation. Therefore, to observe HMGB1 glycosylation, which has been previously reported (Reeves, 1981), we subcloned HMGB1^{WT} DNA into a pFastBac HT-B plasmid and produced HMGB1 protein in insect SF9 cells (insHMGB1^{WT}) for de-glycosylation analysis. HMGB1$^{sig\text{-}pep}$, which has an artificially added signal peptide and was produced in HEK293F cells, was used as a positive control for N-glycosylated HMGB1. Both insHMGB1^{WT} and HMGB1$^{sig\text{-}pep}$ were treated with PNGase F, a glycosidase enzyme that hydrolyzes N-linked oligosaccharides, and then a migration shift analysis was performed. We found that insHMGB1^{WT} was shifted down after enzyme treatment, similar to HMGB1$^{sig\text{-}pep}$, suggesting that HMGB1^{WT} is glycosylated (Fig. 1B). Next, we treated CHO-K1, HeLa and RAW264.7 cells with tunicamycin, an inhibitor of N-linked glycosylation, for 24 h and observed the migration shift of endogenous HMGB1 by western blotting. A band shift of endogenous HMGB1 was observed after tunicamycin treatment (Fig. 1C). Taken together, these data suggest that HMGB1 can be N-glycosylated, confirming a previous report (Reeves, 1981). When RAW264.7 cells were treated with brefeldin A and nocodazole, inhibitors of protein transport from the ER to the Golgi and of microtubule polymerization for vesicular transport, respectively, LPS-stimulated HMGB1 secretion did not decrease (Fig. 1D). These results suggest that the

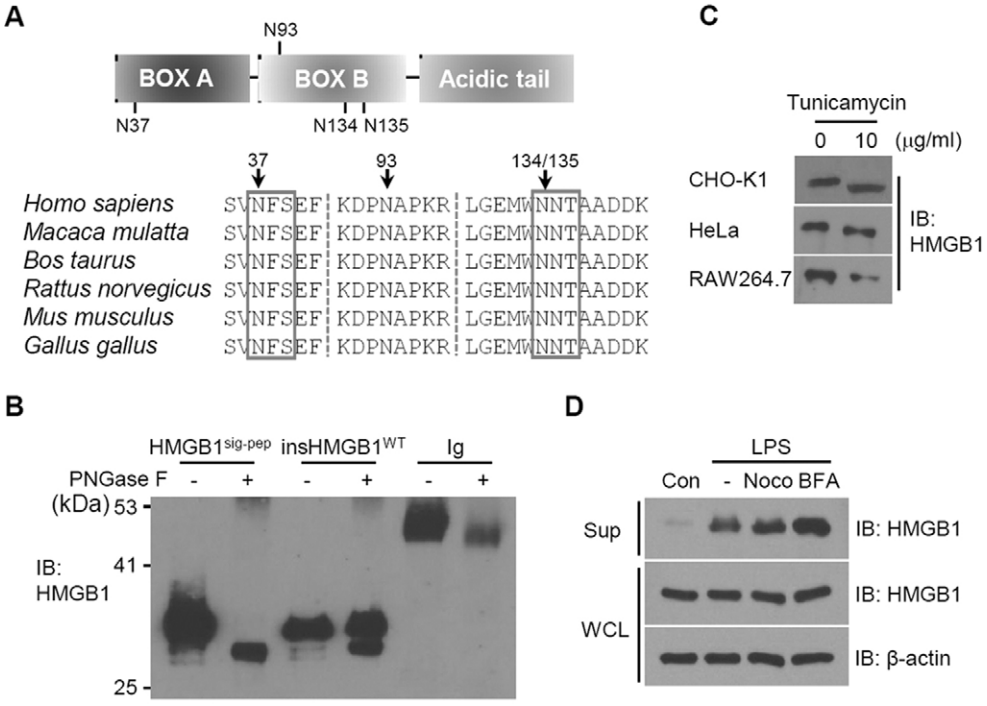

Fig. 1. HMGB1 is N-glycosylated. (A) Four asparagine residues are present in human HMGB1. HMGB1 amino acid sequences of six species, humans, rhesus monkeys, cows, rats, mice and chickens, were compared. Possible N-glycosylation residues were predicted using NetNglyc [NxS/T, http://www.cbs.dtu.dk/services/NetNGlyc/] at N37, N134 and N135, which are boxed. (B) HMGB1$^{sig\text{-}pep}$ and insHMGB1^{WT} were treated with PNGase F overnight at 37°C and immunoblotted with anti-HMGB1 antibody. HMGB1$^{sig\text{-}pep}$ was produced in HEK293F cells, which were transfected with a plasmid containing an HMGB1 with an artificially added signal peptide for ER-targeting in SF9 cells. insHMGB1^{WT} protein was produced in insect SF9 cells transfected with a plasmid containing wild-type HMGB1 without a signal peptide. Ig: immunoglobulin, a positive control glycoprotein. (C) CHO-K1, HeLa and RAW264.7 cells were treated with tunicamycin for 24 h and the migration shift of endogenous HMGB1 was observed by western blotting. (D) RAW264.7 cells were treated with 1 μg/ml LPS for 24 h in the presence or absence of 10 μg/ml of brefeldin A (BFA) and 10 μM nocodazole (Noco), inhibitors of protein transport from the ER to the Golgi and of microtubule polymerization for vesicular transport, respectively, to observe whether HMGB1 was secreted by the conventional secretion pathway. Culture supernatants (Sup) and whole-cell lysates (WCL) were harvested and HMGB1 was immunoblotted (IB) to assess whether it was secreted. Con, medium treated.

Journal of Cell Science (2016) 129, 29-38 doi:10.1242/jcs.176412

conventional ER-Golgi secretion pathway is not related to HMGB1 secretion.

LC-MS/MS analysis of HMGB1

Next, we performed LC-MS/MS analysis of insHMGB1^{WT}. Treatment with PNGase F results in an increase in molecular mass of 0.98 Da over the reference size of HMGB1 peptide fragments. This change is due to the conversion of an asparagine into an aspartic acid residue after a sugar molecule is deleted from the amine group of asparagine by PNGase F (Hao et al., 2010), confirming N-glycosylation in the site. HMGB1 was glycosylated at the N37 and N134 N-glycosylation consensus motifs. Interestingly, N135 is not a typical residue for N-glycosylation, but received a high score of glycosylation, and also displayed the molecular mass change associated with N-glycosylation (Fig. S1A). Next, we compared the molecular shift of insHMGB1^{WT} and insHMGB1$^{N37Q/N134Q}$ by performing western blotting and found that insHMGB1$^{N37Q/N134Q}$ was shifted down compared to insHMGB1^{WT}, suggesting N-glycosylation of HMGB1 (Fig. S1B). We repeated the LC-MS/MS analysis using purified Myc-tagged HMGB1, which was transiently overexpressed in HEK293T cells (Fig. 2A). Approximately 60% of the HMGB1 amino acid sequence was successfully detected and sequenced (Fig. S2A). A peptide including N37 differed between b6 (607.284) and b7 (722.310), and a peptide including N134 and N135 differed between b6 (761.365) and b7 (876.392), and between b7 (875.408) and b8 (990.435), respectively (Fig. 2B; Fig. S2B). We next prepared naturally expressed endogenous HMGB1, and repeated the LC-MS/MS analysis to prove that HMGB1 glycosylation was not limited to the artificial system. We purified endogenous HMGB1 protein from cultured HEK293T cells, using the immunoprecipitation method. The glycan modifications were identified at N37, N134 and N135 residues (Fig. S3). These data show that HMGB1 is N-glycosylated at N37, N134 and N135 as determined by LC-MS/MS analysis.

Analysis of N-linked glycans from HMGB1

We next performed an LC-MS/MS analysis of the glycan structures of HMGB1. Myc–HMGB1 was purified from HEK293T cells transfected with myc–HMGB1 plasmid. A total ion chromatogram of Rapifluor-labeled glycans from 15 µg HMGB1 released by PNGase F was separated using an amide HILIC column. An analysis of glycan profiling of human Ig was used as a test control (data not shown). The chromatogram of the glycans eluted for 22 min was analyzed, where glycan composition and the proposed structures of glycans can be suggested according to the elution time (Fig. 3).

HMGB1 N-glycosylation is crucial for nucleocytoplasmic translocation and secretion of HMGB1

Next, we tested the functional role of HMGB1 N-glycosylation. HMGB1 is translocated to the cytoplasm when modified by acetylation, phosphorylation or oxidation. Therefore, we prepared expression plasmids for EGFP-tagged HMGB1^{WT}, HMGB1$^{N37Q/N134Q}$ and HMGB1$^{N37Q/N135Q}$, and transiently overexpressed these proteins in HEK293T cells to observe their translocation and extracellular secretion. All HMGB1^{WT} was located in the nuclei in the resting state and over 80% was translocated to the cytoplasm upon treatment with trichostatin A (TSA; to induce acetylation), phorbol 12-myristate 13-acetate (PMA; to induce phosphorylation) or H_2O_2 (to induce oxidation) (Fig. 4A),

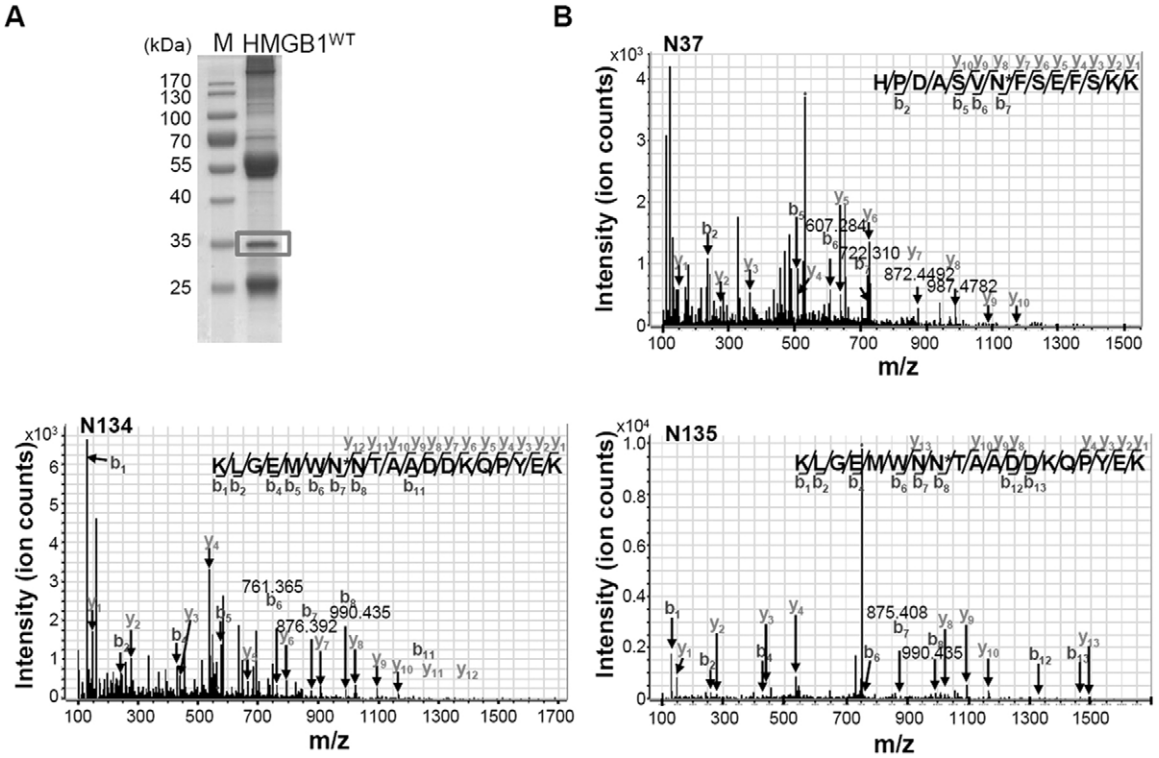

Fig. 2. LC-MS/MS analysis of HMGB1 N-glycosylation. (A) HEK293T cells transiently overexpressing Myc-tagged HMGB1^{WT} were immunoprecipitated with anti-Myc antibody for Coomassie Blue staining. Purified Myc-tagged HMGB1 (box) was extracted for analysis. M, marker. (B) LC-MS/MS analysis of purified Myc-tagged HMGB1, which was transiently overexpressed in HEK293T cells. A peptide including N37 differed between b6 and b7, and N134 and N135 differed between b6 and b7, and between b7 and b8, respectively.

Journal of Cell Science (2016) 129, 29-38 doi:10.1242/jcs.176412

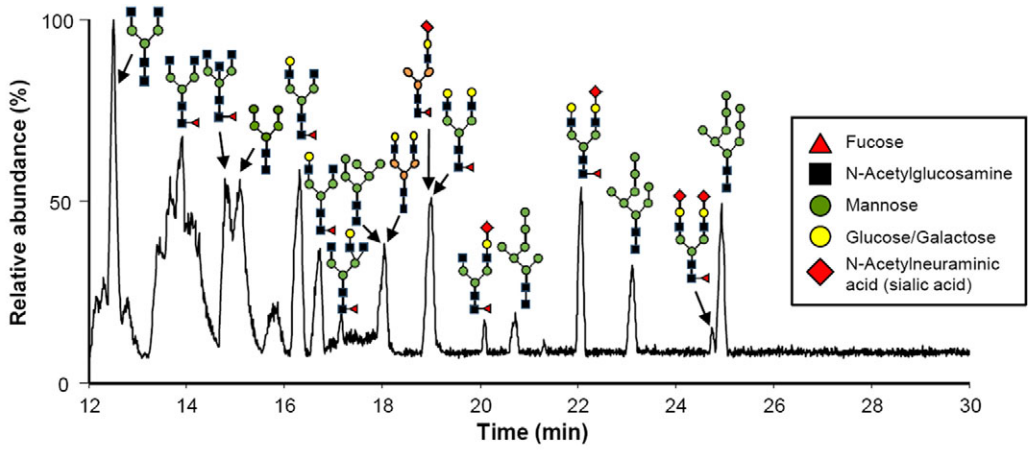

Elution time (min)	Glycan composition	Proposed structure
12.76	$Hex_3HexNAc_4$	
13.91	$Hex_3HexNAc_4Fuc_1$	
15.07	$Hex_3HexNAc_5Fuc_1$	
15.2	$Hex_5HexNAc_2$	
16.31/16.73	$Hex_4HexNAc_4Fuc_1$	
17.14	$Hex_4HexNAc_5Fuc_1$	
18.04	$Hex_6HexNAc_2$	
18.13	$Hex_5HexNAc_4$	

Elution time (min)	Glycan Composition	Proposed structure
18.97	$Hex_4HexNAc_3NeuAc_1Fuc_1$	
19.01	$Hex_5HexNAc_4Fuc_1$	
20.09	$Hex_4HexNAc_4NeuAc_1Fuc_1$	
20.72	$Hex_7HexNAc_2$	
22.07	$Hex_5HexNAc_4NeuAc_1Fuc_1$	
23.13	$Hex_8HexNAc_2$	
24.75	$Hex_5HexNAc_4NeuAc_2Fuc_1$	
24.92	$Hex_9HexNAc_2$	

Fig. 3. Profiling of N-linked glycans from HMGB1. Myc–HMGB1 was purified from HEK293T cells transfected with Myc–HMGB1 plasmid. A total ion chromatogram of Rapifluor-labeled glycans from 15 µg HMGB1 released by PNGase F was separated by an amide HILIC column. Structural assignments are based on monosaccharide composition and fragmentation analyses. The sugar symbols are those following the Consortium for Functional Glycomics (http://www.functionalglycomics.org).

confirming previous results (Bonaldi et al., 2003; Hoppe et al., 2006; Youn and Shin, 2006). However, the cytoplasmic translocation of EGFP–HMGB1$^{N37Q/N134Q}$ and EGFP–HMGB1$^{N37Q/N135Q}$ was severely decreased, to 20% and 40%, respectively, even after treatment with TSA, PMA or H_2O_2 (Fig. 4B–D).

We next observed the extracellular secretion of HMGB1 (Fig. 4E). When HEK293T cells were transfected with EGFP–HMGB1^{WT} plasmid, EGFP–HMGB1^{WT} secretion was profoundly increased upon treatment with PMA, TSA and H_2O_2. However, when transfected with the double mutants HMGB1$^{N37Q/N134Q}$ and HMGB1$^{N37Q/N135Q}$, their secretion was barely detectable even after treatment with TSA, PMA or H_2O_2. When the cells were transfected with single mutants HMGB1^{N37Q}, HMGB1^{N134Q} or HMGB1^{N135Q}, HMGB1 secretion was partially decreased after stimulation. When we treated J774A.1 cells with LPS for 24 h or starved the cells (Fig. 4F), the secretion patterns of HMGB1^{WT} and mutant proteins were similar. These data suggest that HMGB1 N-glycosylation at N37, N134 and N135 is a prerequisite for nucleocytoplasmic translocation and secretion of HMGB1.

HMGB1 has improved mobility in the nucleus and improved nuclear export upon N-glycosylation

HMGB1 is located in the nucleus under resting conditions and binds to the minor groove of DNA; this binding ability is reduced by methylation (Ito et al., 2007). We next tested whether N-glycosylation of HMGB1 influences its movement in the nuclei of live HEK293T cells by using FRAP analysis. FRAP data indicate the rate at which fluorescent molecules exchange with photobleached molecules. The recovery percentage of fluorescence in the area of photobleaching will decrease if the protein mobility is decreased. The recovery percentages of EGFP-tagged HMGB1$^{N37Q/N134Q}$ and HMGB1$^{N37Q/N135Q}$ were lower than that of EGFP–HMGB1^{WT} within 4 s, suggesting slower mobility (Fig. 5A). Therefore, we hypothesized that HMGB1 N-glycosylation influences its DNA binding. In order to test this, plasmid DNA was incubated with insHMGB1^{WT} and insHMGB1$^{N37Q/N134Q}$, and complex formation was observed. As shown in Fig. 5B, the migration of complexes of insHMGB1$^{N37Q/N134Q}$ and plasmid DNA were retarded compared

Journal of Cell Science (2016) 129, 29-38 doi:10.1242/jcs.176412

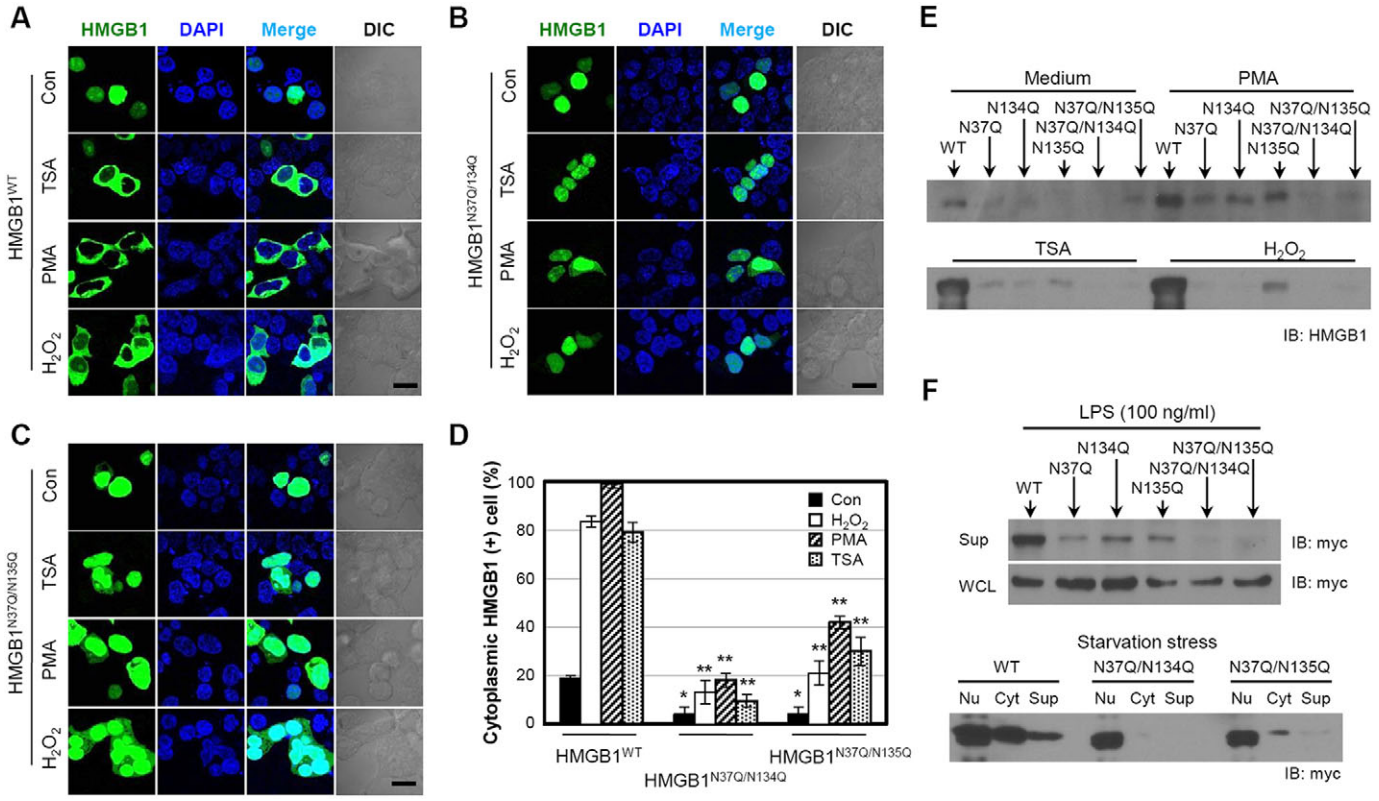

Fig. 4. Effect of HMGB1 N-glycosylation on intracellular movement and secretion of HMGB1. (A–C) Movements of EGFP–tagged HMGB1^{WT}, mutant HMGB1$^{N37Q/N134Q}$ and HMGB1$^{N37Q/N135Q}$ in HEK293T cells. HEK293T cells were transfected with each plasmid for 48 h and then treated with 10 ng/ml TSA for 2 h, 250 nM PMA for 4 h or 50 µM H_2O_2 for 2 h. The movements of EGFP–HMGB1 were observed under a confocal microscope. (D) The localization of HMGB1-EGFP (+) was recorded in 80 cells from the experiments described in A–C to determine the localization of HMGB1. Results are mean±s.e.m. *P<0.01, **P<0.001 compared to HMGB1^{WT} (Student's t-test). (E) HEK293T cells were transfected with the indicated EGFP-tagged HMGB1 plasmids for 24 h and then treated with PMA, TSA or H_2O_2 for 18 h. Culture supernatants were harvested and immunoblotted (IB) to detect HMGB1. (F) J774A.1 cells were transfected with Myc-tagged EGFP-HMGB1 plasmids for 24 h and then treated with 100 ng/ml LPS for 24 h. For starvation, cells were cultured in EBSS for 4 h. Culture supernatants were collected and immunoblotted with anti-HMGB1 or anti-Myc antibodies to observe HMGB1 secretion. Nu, nucleus; Cyt, cytoplasm; Sup, supernatant.

to those of insHMGB1^{WT}, and some complexes did not migrate and remained in the wells. The effect of HMGB1 N-glycosylation on binding between the N-acetyl-D-glucosamine (GlcNAc)-tagged HMGB1 A or B box and double-stranded DNA (dsDNA) was modeled using the structures of the complexes of HMGB1 A box and B box bound to dsDNA as templates (PDB ID 1CKT and 2GZK, respectively) (Stott et al., 2006; Watson et al., 2007). As shown in Fig. 5C, HMGB1 GlcNAc molecules at N37 and N134 induce steric hindrance on binding between HMGB1 and dsDNA. Although the carbohydrate chains are flexible, they could interfere with the phosphate backbone or the nucleic acids of the dsDNA. As seen in Fig. 5C, only two GlcNAc molecules linked by a glycosidic bond were drawn instead of entire carbohydrate chains for clarity.

N-glycosylated HMGB1 has improved binding to CRM1 compared to non-glycosylated HMGB1

Nuclear HMGB1 is translocated to the cytoplasm after binding to the nuclear exportin CRM1 (Bonaldi et al., 2003); hence, we tested the binding of each mutant HMGB1 protein to CRM1. HEK293T cells were co-transfected with CRM1 plasmid and either Myc-tagged HMGB1^{WT}, HMGB1$^{N37Q/N134Q}$ or HMGB1$^{N37Q/N135Q}$ for 48 h, and then treated with 10 ng/ml TSA for 4 h to observe the effect of HMGB1 acetylation. The cells were lysed and immunoprecipitated with anti-Myc antibody and then immunoblotted with CRM1. As shown in Fig. 6, myc–HMGB1^{WT} binding to CRM1 increased after TSA treatment, as previously described (Bonaldi et al., 2003). HMGB1$^{N37Q/N134Q}$ and HMGB1$^{N37Q/N135Q}$ binding to CRM1 were profoundly decreased when compared with HMGB1^{WT}. These results suggest that HMGB1 N-glycosylation is important for binding to CRM1 and, thus, also for HMGB1 secretion.

Protein stability of de-glycosylated HMGB1 mutant proteins

Protein glycosylation is important in protein structure and stability. Therefore, we tested the effect of glycosylation on the intracellular stability of HMGB1 using HMGB1$^{N37Q/N134Q}$ and HMGB1$^{N37Q/N135Q}$ plasmids. HEK293T cells were transfected with HMGB1^{WT}, HMGB1$^{N37Q/N134Q}$ or HMGB1$^{N37Q/N135Q}$ plasmids and then treated with cycloheximide (CHX) to inhibit protein translation and observe protein stability. Cells were harvested and HMGB1 protein levels were analyzed by western blotting. HMGB1^{WT} protein levels were fairly consistent and decreased by only 10% after 48 h. However, HMGB1$^{N37Q/N134Q}$ and HMGB1$^{N37Q/N135Q}$ levels decreased by 60% and 30%, respectively, after 48 h (Fig. 7A). These data suggest that HMGB1 is degraded quickly when not properly glycosylated. HEK293T cells were then transfected with HMGB1^{WT} or HMGB1$^{N37Q/N134Q}$ plasmids for 24 h and treated with a proteasome inhibitor, MG132, in the presence or absence of 20 mM NH_4Cl, a lysosomal inhibitor that prevents protease activity. No significant change was observed in HMGB1^{WT} protein levels, but a dramatic recovery of HMGB1$^{N37Q/N134Q}$ was

Journal of Cell Science (2016) 129, 29-38 doi:10.1242/jcs.176412

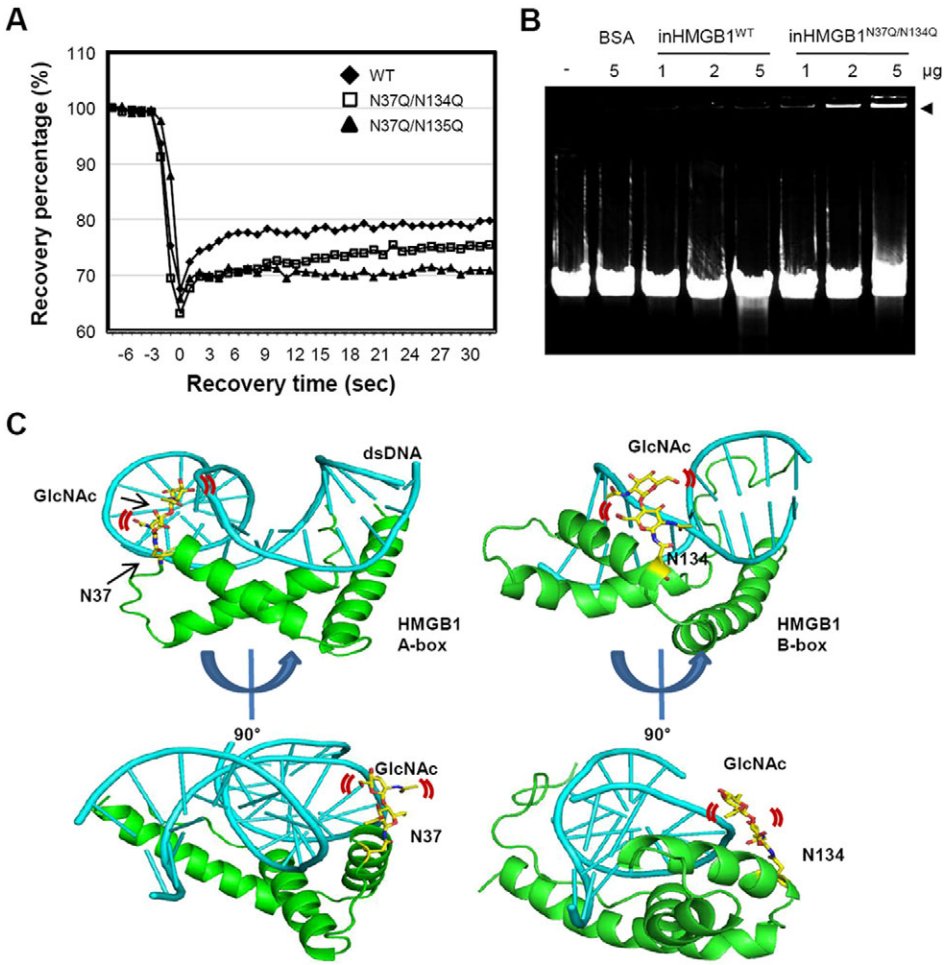

Fig. 5. DNA-binding ability of N-glycosylated HMGB1. (A) FRAP analysis of HMGB1^{WT}, HMGB1$^{N37Q/N134Q}$ and HMGB1$^{N37Q/N135Q}$. HEK293T cells were transfected with EGFP-tagged HMGB1 plasmids for 48 h, followed by photobleaching of the nucleus and measurement of the percentage recovery of fluorescence to determine protein mobility. The experiment was repeated four times, and the mean values are shown. (B) DNA binding of HMGB1^{WT} and HMGB1$^{N37Q/N134Q}$. HMGB1^{WT} and HMGB1$^{N37Q/N134Q}$ proteins were incubated with plasmid DNA for 2 h at 37°C and DNA migration was analyzed on a 1% agarose gel. BSA, negative control protein. The arrowhead indicates non-migrating plasmid-DNA–HMGB1 protein complexes in the wells. Data represent one of two or four similar independent experiments in A and B, respectively. (C) A modeling study between GlcNAc-tagged HMGB1 A and B boxes at N37 and N134, respectively, and dsDNA as templates using the WinCoot program. Illustration represents the HMGB1 A or B box (green) and dsDNA (cyan) complex structure. Two GlcNAc molecules are shown as yellow stick models. The cartoon or stick structures were produced by the PyMOL program (http://www.pymol.org).

observed upon treatment with MG132 (Fig. 7B), suggesting that HMGB1$^{N37Q/N134Q}$ is degraded in a proteasome-mediated pathway. In addition, HMGB1$^{N37Q/N134Q}$ and HMGB1$^{N37Q/N135Q}$ were ubiquitylated at K48, which is a degradation signal (Fig. 7C). These results suggest that HMGB1 glycosylation is important for HMGB1 stability.

DISCUSSION

HMGB1 secretion is modulated by the PTMs of acetylation, phosphorylation, methylation and oxidation, which drive HMGB1 to the cytoplasm and then to the extracellular space through an unconventional secretion pathway. Although it has no signal peptide, a low degree of glycosylation of HMGB1 has been reported previously (Reeves and Chang, 1983; Elton and Reeves, 1986; Chao et al., 1994), but the significance of glycosylation and the glycosylation residue had not been identified.

In this study, we demonstrated that HMGB1 could be glycosylated by performing a gel shift analysis after PNGaseF treatment and a tunicamycin-mediated N-glycosylation inhibition assay. LC-MS/MS analysis showed that there were two N-glycosylations at N37 and N134, at NxS/T consensus motifs, and one at the non-classical consensus residue N135, in recombinant HMGB1 proteins produced in both HEK293T and insect cells. Recently, the sequence requirements of the acceptor substrate for N-glycosylation have become less strict and it has been shown that atypical (non-consensus) N-linked glycosylation is possible (Valliere-Douglass et al., 2010; Schwarz and Aebi, 2011). Previously, it had been reported that HMGB1 contains a low degree of glycosyl modification in calf thymus (Reeves et al., 1981; Reeves and Chang, 1983; Elton and Reeves, 1986; Chao et al., 1994), and our data confirmed this glycosylation and identified the glycosylation residues. In addition, recombinant HMGB1 expressed in CHO cells treated with glycopeptidase F resulted in the removal of an N-linked oligosaccharide (Li et al., 2004), and the HMG family proteins HMGN1 and HMGN2 are also N-glycosylated (Reeves and Chang, 1983). Taken together, these results suggest that HMGB1 is N-glycosylated.

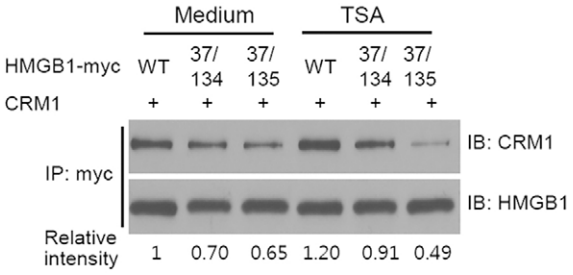

Fig. 6. Effect of HMGB1 N-glycosylation on CRM1 binding. HEK293T cells were co-transfected with Myc-tagged HMGB1^{WT}, HMGB1$^{N37Q/N134Q}$ (37/134) or HMGB1$^{N37Q/N135Q}$ (37/135), and CRM1 plasmids for 48 h, and then treated with 10 ng/ml TSA for 4 h. Cell lysates were immunoprecipitated (IP) with anti-Myc antibody and then immunoblotted (IB) with anti-CRM1 antibody. The relative density was than calculated. Data represent one of three similar independent experiments.

Journal of Cell Science (2016) 129, 29-38 doi:10.1242/jcs.176412

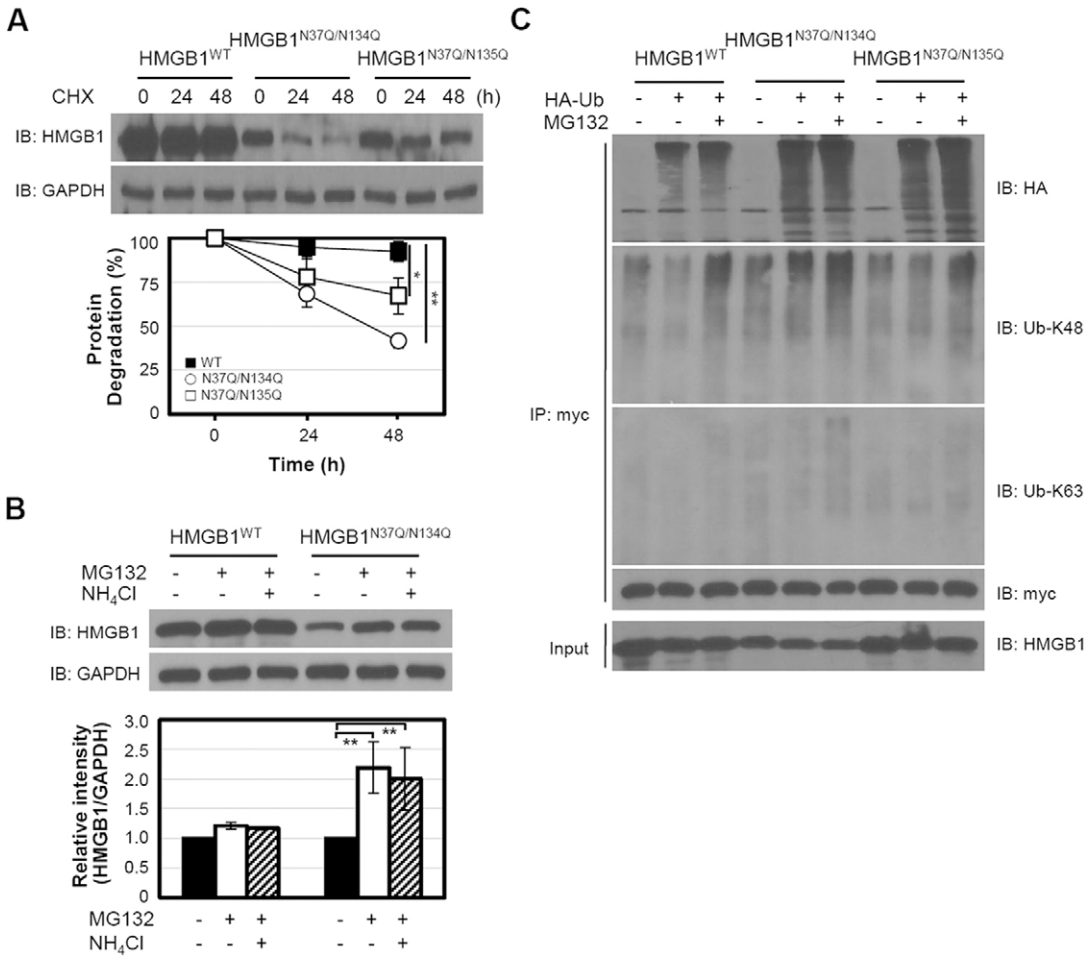

Fig. 7. Stability of glycosylated HMGB1. (A) HEK293T cells were transfected with HMGB1^{WT}, HMGB1$^{N37Q/N134Q}$ and HMGB1$^{N37Q/N135Q}$ plasmids and then treated with 70 µg/ml cycloheximide (CHX) to observe protein degradation. HMGB1 levels were analyzed by western blotting to determine the protein degradation rate. The experiment was repeated four times. Results are mean±s.e.m. *P<0.01, **P<0.001 (Student's t-test). (B) HEK293T cells were transfected with each HMGB1 plasmid for 24 h, and then treated with 10 µM MG132 in the presence or absence of 20 mM NH_4Cl. Cell lysates were immunoblotted with anti-HMGB1 antibody, and the relative intensity of HMGB1 compared to GAPDH was measured. The experiment was repeated three times. Results are mean±s.e.m. **P<0.001 (Student's t-test). (C) HEK293T cells were co-transfected with Myc-tagged HMGB1 and HA–ubiquitin (Ub) plasmids and immunoprecipitated (IP) with anti-Myc antibody. Immunoblot (IB) analyses were performed to observe HMGB1 ubiquitylation at K48, which signals degradation.

The significance of HMGB1 glycosylation was not known, even though HMGB1 glycosylation was reported over 20 years ago. Here, we show that HMGB1 N-glycosylation is required for nucleocytoplasmic translocation and extracellular secretion. When HEK293T cells transfected with HMGB1$^{N37Q/N134Q}$ or HMGB1$^{N37Q/N135Q}$ plasmid were treated with PMA, TSA or H_2O_2, the mutant HMGB1 primarily showed nuclear localization with a profound reduction in extracellular secretion. These results demonstrate that the PTMs of acetylation, phosphorylation and oxidation are not sufficient for HMGB1 secretion, and glycosylation is a prerequisite for HMGB1 translocation. Based on the results showing that HMGB1$^{N37Q/N134Q}$ and HMGB1$^{N37Q/N135Q}$ had stronger binding to nuclear DNA and weaker binding to CRM1 compared to HMGB1^{WT}, we suggest that HMGB1 N-glycosylation at N37, N134 and N135 is important for HMGB1 intracellular trafficking and secretion.

N-glycans are synthesized and transferred to polypeptides containing a signal peptide, by glycosyltransferase, at aspargine residues within the NxS/T sequon on the luminal side of the ER and Golgi (Molinari, 2007; Hebert et al., 2014). However, the mechanism by which HMGB1 becomes glycosylated despite being devoid of signal peptide is still is unknown, as N-glycosylation rarely exists in the cytosol. Based on a molecular mass shift upon PNGase F treatment, as analyzed by western blot and profiling of N-glycans, some amount of glycosylation is linked to HMGB1.

The secretion of protein devoid of signal peptide is not fully understood as the protein is unable to access the conventional secretion pathway through the ER. IL-1β is a model protein without a signal peptide and with an unconventional secretion pathway based on the autophagy mechanism, an important pathway for extracellular delivery (Dupont et al., 2011). Autophagy has recently been shown to regulate selective HMGB1 secretion in dying tumor cells (Thorburn et al.l, 2009). An investigation of the interaction of autophagy-based unconventional secretion of HMGB1 and HMGB1 glycosylation is needed to further identify and understand the pathophysiologic mechanism of HMGB1-mediated inflammation. In summary, HMGB1 can be N-glycosylated at N37 and either at residue N134 or N135, and this determines the nucleocytoplasmic transport, extracellular secretion and protein stability of HMGB1.

Journal of Cell Science (2016) 129, 29-38 doi:10.1242/jcs.176412

MATERIALS AND METHODS

Cell culture, transfection and reagents

Human embryonic kidney (HEK) 293T, Chinese hamster ovary (CHO)-K1 cells and HeLa cells were cultured in Dulbecco's modified Eagle's medium (DMEM) supplemented with 10% fetal bovine serum (FBS, Life Technologies), 100 U/ml penicillin, 100 µg/ml streptomycin and 2 mM L-glutamine at 37°C under 5% CO_2. Mouse macrophage cell lines J774A.1 and RAW264.7 were cultured in RPMI1640 medium supplemented with the reagents described above. Plasmid transfection was carried out using Fugene HD reagent (Promega) as recommended by the manufacturer. HEK293T cells were treated for 18 h with 15 ng/ml histone deacetylase inhibitor trichostatin A (TSA, Sigma-Aldrich), 250 nM phorbol 12-myristate 13-acetate (PMA, Sigma-Aldrich) and 20 µM H_2O_2 (Sigma-Aldrich), to induce acetylation, phosphorylation and oxidation, respectively. Proteasome inhibitor MG132 (0.5 µM, Sigma-Aldrich) and protein biosynthesis inhibitor cycloheximide (CHX) (70 µg/ml, Sigma-Aldrich), were also used. J774A.1 cells were treated with 100 ng/ml LPS (*E. coli* 0111:B4, Sigma-Aldrich) for HMGB1 secretion. Tunicamycin (10 µg/ml, Sigma-Aldrich) was used for inhibition of N-glycosylation in HeLa, RAW264.7 and CHO-K1 cells.

Plasmids and *in situ* mutagenesis

Myc- and enhanced green fluorescent protein (EGFP)-tagged $HMGB1^{WT}$ and HMGB1 glycosylation mutant genes were inserted into the pCMV plasmid for mammalian cell expression. Site-directed mutations of HMGB1 were generated utilizing pFastBac HT-B-HMGB1 as a template using the QuikChange site-directed mutagenesis kit (Stratagene). Three asparagine residues, N37, N134 and N135 were single or doubly mutated to glutamine: HMGB1 N37Q, N134Q, N135Q, N37Q/N134Q, or N37Q/N135Q. The sequences of primers used for construction of human HMGB1 mutants are as follows: HMGB1 N37Q, 5′-CAGATGC-TTCAGTCAATTCTCAGAGTTTTC-3′ (forward) and 5′-GAAAACTCT-GAGAATTGGACTGAAGCATCTG-3′ (reverse); HMGB1 N134Q, 5′-AGAGATGTGGCAAAACACTGCTGCA-3′ (forward) and 5′-TGCA-GCAGTGTTTTGCCACATCTCT-3′ (reverse); and HMGB1 N135Q, 5′-AGATGTGGAATCAAACTGCTGCAGATG-3′ (forward) and 5′-CATC-TGCAGCAGTTTGATTCCACATCT-3′ (reverse).

Recombinant HMGB1 cloning, expression and purification

An *Eco*RI–*Xho*I fragment containing full-length $HMGB1^{WT}$ and $HMGB1^{N37Q/N134Q}$ ($insHMGB1^{WT}$ and $insHMGB1^{N37Q/N134Q}$) were cloned into pFastBac HT-B, and recombinant baculovirus was produced according to the manufacturer's manual (Invitrogen). The N-terminus six histidine (6× His)-containing HMGB1 WT and N37Q/N134Q plasmids were expressed by SF9 cells for 36 h. The insect cells were then purified on a Ni-NTA column (GE Healthcare) with lysis buffer (25 mM Tris-HCl pH 7.5, 300 mM NaCl, 10% glycerol, 30 mM imidazole, 5 mM β-mercaptoethanol). HMGB1 was then eluted with elution buffer (25 mM Tris-HCl pH 7.5, 300 mM NaCl, 10% glycerol, 300 mM imidazole, 5 mM β-mercaptoethanol). After tobacco etch virus (TEV) protease treatment for 16 h at 4°C, size exclusion chromatography (Superdex-200 column, GE Healthcare) was carried out under buffer containing 25 mM Tris-HCl pH 7.5 and 150 mM NaCl to verify protein homogeneity.

Western blot analysis and immunoprecipitation

HEK293T cells in six-well plates were transfected with various combinations of plasmids using Fugene HD. For immunoblotting, cells were washed with phosphate-buffered saline (PBS) and lysed in 1× radioimmunoprecipitation assay (RIPA) buffer (GenDEPOT) containing 150 mM NaCl, 1% Triton X-100, 1% deoxycholic acid sodium salt, 0.1% sodium dodecyl sulfate (SDS), 50 mM Tris-HCl pH 7.5, 2 mM EDTA and protease inhibitor cocktail. Whole-cell lysates were centrifuged at 20,000 ***g*** for 10 min at 4°C. Protein sample buffer was added to the whole-cell lysates (100 mM Tris-HCl pH 6.8, 2% SDS, 25% glycerol, 0.1% bromophenol blue, and 5% β-mercaptoethanol) followed by heating at 94°C for 5 min. In all experiments, 20 µg protein were separated by molecular mass through SDS-PAGE and transferred onto nitrocellulose membranes (GE Healthcare). Non-specific binding sites were blocked by incubating the membranes in Tris-buffered saline (TBS) supplemented with 0.1% Tween 20 and 5% (w/v) low-fat milk for 1 h. Anti-HMGB1 (Abcam; ab18256, rabbit antibody against the region from amino acid 150 to the C-terminus of HMGB1), anti-CRM1 and anti-HA (Santa Cruz Biotechnology), anti-glyceraldehyde 3-phosphate dehydrogenase (GAPDH, AbFrontier), anti-ubiquitin-K63 and -K48 (Millipore), and anti-c-Myc (Invitrogen Technology) antibodies were used. Membranes were washed three times for 10 min each with TBS with 0.1% Tween 20 (TBST), probed with the appropriate horseradish peroxidase (HRP)-conjugated secondary antibody for 1 h, and washed three times for 10 min each with TBST. Enhanced chemiluminescent (ECL) substrate (GenDEPOT) was then used for visualization. Membranes were then stripped by submerging in stripping buffer (50 mM glycine, pH 2.2) at room temperature for 1 h under constant shaking.

Immunoprecipitation was performed with 200 µg protein, which was pre-cleared with 20 µl of protein G beads (Sigma-Aldrich) for 1 h at 4°C, followed by overnight incubation with 1 µg of the specific antibody. The next day, samples were added to 20 µl of protein G beads and rotated at 4°C for 2 h. The beads were then washed three times with ice-cold PBS, and then mixed with protein sample buffer followed by heating at 94°C for 5 min. The proteins were separated using SDS-PAGE.

A deglycosidase assay was performed to determine HMGB1 de-glycosylation. Recombinant HMGB1 proteins $HMGB1^{sig\text{-}pep}$ and $insHMGB1^{WT}$ were resuspended in 20 mM ammonium bicarbonate buffer (pH 8.0) and boiled for 10 min at 98°C. $HMGB1^{sig\text{-}pep}$ (A&RT) was produced in HEK293F cells by adding an ER-targeting Ig signal peptide to HMGB1 (Leahy et al., 1988). The proteins were then treated with PNGase F and incubated overnight at 37°C. Proteins were separated using SDS-PAGE for western blotting.

RAW264.7 cells (1×10^6 cells/well) were treated with 1 µg/ml of LPS in the presence of 10 µg/ml of brefeldin A and 10 µM nocodazole (Sigma-Adrich) for 24 h to see whether HMGB1 was secreted by the conventional secretion pathway. Culture supernatants and whole-cell lysates were harvested, and HMGB1 was immunoblotted for HMGB1 secretion.

LC-MS/MS for peptide analysis

HMGB1 protein was purified from HEK293T cells transfected with a Myc–HMGB1 plasmid for 48 h. Cells were lysed with 1× RIPA buffer and then protein G beads conjugated with anti-Myc antibody were added to the lysates. Beads were rotated at 4°C overnight and then washed three times with ice-cold PBS. Samples were mixed with protein sample buffer, boiled at 94°C for 5 min, and then separated using SDS-PAGE followed by Coomassie Blue staining. The HMGB1 band was extracted from the gel for analysis. Endogenous HMGB1 protein was prepared from whole-cell lysate of HEK293T cells to detect the presence of N-glycosylated residues in naturally expressed HMGB1. Whole-cell lysate was immunoprecipitated with anti-HMGB1 antibody conjugated to protein G beads, which were pre-cleared.

HMGB1 proteins were treated with PNGase F for LC-MS/MS analysis. LC-MS/MS analysis was performed with a nano high performance liquid chromatography (HPLC) system (Agilent) using the nano chip column (150 mm×0.075 mm) for peptide separation. Mobile phase A for liquid chromatography separation was 0.1% formic acid in deionized water and mobile phase B was 0.1% formic acid in acetonitrile. The chromatography gradient was designed for a linear increase from 5% B to 30% B in 25 min, 40% B to 60% B in 5 min, 90% B in 10 min, and 5% B in 15 min. The flow rate was maintained at 300 nl/min. Product ion spectra were collected in the information-dependent acquisition (IDA) mode and were analyzed by Agilent 6530 Accurate-Mass quadrupole time-of-flight (Q-TOF) using continuous cycles of one full scan TOF mass spectrometry reading from 200–1500 *m*/*z* (1.0 s) plus three product ion scans from 50–1800 m/z (1.5 s each). Precursor *m*/*z* values were selected starting with the most intense ion and using a selection quadrupole resolution of 3 Da. The rolling collision energy feature was used, which determines collision energy based on the precursor value and charge state. The dynamic exclusion time for precursor ion *m*/*z* values was 60 s. The mascot algorithm (Matrixscience) was used to identify peptide sequences present in a protein sequence database. Mascot searches against an in-house database of HMGB1 (Genbank accession no.

CAG33144.1) were performed with the following criteria: fixed modification, carboxyamidomethylated at cysteine residues, variable modification, oxidized at methionine residues, deamidation at aspartic acid and asparagine, maximum allowed missed cleavage of 2, mass spectrometry tolerance of 100 ppm, and MS/MS tolerance of 0.1 Da. Only peptides resulting from trypsin digests were considered.

Profiling of HMGB1 N-glycans

For the HMGB1 N-glycan analysis, HEK293T cells were transfected with myc–HMGB1 plasmid for transient expression. Whole-cell lysate was prepared and the protein supernatant was applied to the affinity column of a c-Myc tag immunoprecipitation or co-immunoprecipitation kit (Pierce). The purity of myc–HMGB1 was confirmed to be sufficient by analyzing for N-glycans. A total of 15 µg of myc–HMGB1 protein was treated with PNGase F and then labeled with RapiFlour reagent (Waters). The final solution was diluted with acetonitrile for HILIC enrichment. The glycan enrichment was performed with a Waters GlycoWorks™ HIULIV µElution Plate, based on the manufacturer's protocol. Briefly, the well was washed with 200 µl of deionized water and primed with 200 µl of 85% acetonitrile. Then, the labeled glycan sample was loaded to the well and washed with 2×600 µl of 1:9:90 (v/v/v) formic acid:water:acetonitrile solution. Finally, the glycans were eluted with 3×30 µl of 200 mM ammonium acetate in 5% acetonitrile. The enriched glycan was injected onto the ACQUITY I UPLC Glycan BEH amide column (2.1 mm×150 mm, 1.7 µm particle size, Waters). Separation was performed with eluent A, consisting of 50 mM ammonium formate, and eluent B, consisting of 100% acetonitrile, with a 35-min liner gradient from 25% to 46% eluent A at a flow rate of 0.4 ml/min. The effluent was electro-sprayed into the LTQ Elite (Thermo). Blanks were run prior to the sample run to ensure that there were no significant signals from the solvents or the column. A database search was carried out using a SimGlycan algorithm (SimGlycan v5.0).

Confocal microscopy

In order to observe nuclear–cytoplasmic translocation of HMGB1 in HEK293T cells under various stimulation conditions, HEK293T cells were transfected with EGFP-tagged $HMGB1^{WT}$ and mutant plasmids and cultured on cover glass in a six-well plate. After 48 h, cells were treated with 50 µM H_2O_2 for 2 h, 250 µM PMA for 4 h and 10 ng/ml TSA for 2 h. Cells were fixed with 4% paraformaldehyde-PHEM buffer (60 mM PIPES, 25 mM HEPES, 10 mM EGTA and 4 mM $MgSO_4$, pH 7.0) for 20 min at room temperature and washed with cold PBS. After mounting with 4′,6′-diamidino-2-phenylindole (DAPI), cells were observed with a confocal FV1000 microscope (Olympus).

Nuclear and cytosolic fractionation

Nuclear and cytosolic fractionation was performed using a nuclear and cytosolic fractionation kit (BioVision). HEK293T cells in six-well plates were transfected with HMGB1 WT, N37Q/N134Q or N37Q/N135Q plasmids and incubated for 48 h. Cells were incubated with Earle's balanced salt solution (EBSS) for 4 h to induce starvation and then harvested by centrifugation at 600 ***g*** for 5 min at 4°C. Samples were added to 0.2 ml cytosol extraction buffer (CEB)-A containing dithiothreitol (DTT) and protease inhibitors. Samples were vigorously vortexed for 15 s to fully resuspend the cell pellet, and then incubated on ice for 10 min followed by addition of 11 µl of ice-cold CEB-B. Samples were vortexed for 5 s, incubated on ice for 10 min and then centrifuged for 5 min at 16,000 ***g***. The supernatant fraction (cytoplasmic extraction) was then transferred to a clean pre-chilled tube. The pellets containing the nuclei were resuspended in 100 µl of ice-cold nuclear extraction buffer (NEB) mixture, vortexed for 15 s, returned to ice and vortexed for 10 min, and then centrifuged at 16,000 ***g*** for 10 min. The supernatant (nuclear extract) was immediately transferred to a clean pre-chilled tube.

Gel mobility shift assay

In order to observe the DNA binding of wild-type and mutant HMGB1 proteins, a gel retardation assay was performed. Plasmid DNA was prepared by *Eco*RI digestion and then purified. Recombinant $HMGB1^{WT}$ and $HMGB1^{N37Q/N134Q}$ were then incubated with plasmid DNA at 37°C for 2 h and migration was analyzed on a 1% agarose gel.

FRAP

A FRAP assay was performed to analyze the binding of HMGB1 to nuclear DNA within the nucleus by measuring the mobility of HMGB1. HEK293T cells were seeded on covered glass-bottom dishes and transfected with GFP-tagged HMGB1 WT, N37Q/N134Q or N37Q/N135Q plasmids for 48 h. Transfected cells were viewed under a confocal FV1000 fluorescent microscope and bleached using laser diode at 405 nm at 90% for 3 s. The nuclei were then scanned to measure the recovery rate of GFP fluorescence by region optical intensity (ROI) value. FRAP graphs were created using Liveplot.

Modeling of N-glycosylated HMGB1 structure *in silico*

In order to draw a model of the N-glycosylated HMGB1 structure, we used the complex structures of HMGB1 A box and B box bound to dsDNA as templates (PDB ID 1CKT and 2GZK, respectively). Two N-acetyl-D-glucosamine (GlcNAc) molecules, which are the first two sugars of glycosylation, were manually attached to HMGB1 N37 and N134 using the WinCoot program (Emsley and Cowtan, 2004). The cartoon or stick structures were produced by the PyMOL program (PyMOL, http://www.pymol.org).

Statistical analysis

Analysis of experiments was performed with Student's *t*-test using GraphPad Prism. Data represent the mean±s.e.m., as indicated in the individual figure legends. The difference was considered statistically significant when $P<0.05$.

Acknowledgements

We thank Nahee Kim and Young Joo Sun for providing a protocol of HMGB1 protein purification.

Competing interests

The authors declare no competing or financial interests.

Author contributions

Y.H.K. carried out LC-MS/MS analysis, FRAP, confocal microscopy, gel mobility shift analysis, western blot analyses, HMGB1 degradation assay, and drafted the manuscript. M.S.K. participated in identification of N-glycosylation, plasmid constructions of WT and mutant HMGB1 and CRM1, and protein production. J.B.P. performed production of HMGB1 protein from insect cells and modeling of N-glycosylated HMGB1 structure *in silico*. S.-A.L. participated in HMGB1 secretion test. J.E.C. participated in revision study design and discussion. H.-S.C. and J.-S.S. supervised and coordinated all the experiments. J.-S.S. wrote the manuscript. All authors read and approved the final manuscript.

Funding

This work was supported by the National Research Foundation of Korea (NRF) funded by the Korean government (MEST) [grant numbers 2011-0017611 and 2014R1A4A1008625 to J.-S.S., 2012R1A2A2A01012830 to H.-S.C.].

Supplementary information

Supplementary information available online at
http://jcs.biologists.org/lookup/suppl/doi:10.1242/jcs.176412/-/DC1

References

Bell, C. W., Jiang, W., Reich, C. F., III and Pisetsky, D. S. (2006). The extracellular release of HMGB1 during apoptotic cell death. *Am. J. Physiol. Cell Physiol.* **291**, C1318-C1325.

Boffa, L. C., Sterner, R., Vidali, G. and Allfrey, V. G. (1979). Post-synthetic modifications of nuclear proteins high mobility group proteins are methylated. *Biochem. Biophys. Res. Commun.* **89**, 1322-1327.

Bonaldi, T., Talamo, F., Scaffidi, P., Ferrera, D., Porto, A., Bachi, A., Rubartelli, A., Agresti, A. and Bianchi, M. E. (2003). Monocytic cells hyperacetylate chromatin protein HMGB1 to redirect it towards secretion. *EMBO J.* **22**, 5551-5560.

Chao, Y. B., Scovell, W. M. and Yan, S. B. (1994). High mobility group protein, HMG-1, contains insignificant glycosyl modification. *Protein Sci.* **3**, 2452-2454.

Dimov, S. I., Alexandrova, E. A. and Beltchev, B. G. (1990). Differences between some properties of acetylated and nonacetylated forms of HMG1 protein. *Biochem. Biophys. Res. Commun.* **166**, 819-826.

Dupont, N., Jiang, S., Pilli, M., Ornatowski, W., Bhattacharya, D. and Deretic, V. (2011). Autophagy-based unconventional secretory pathway for extracellular delivery of IL-1β. *EMBO J.* **30**, 4701-4711.

Einck, L. and Bustin, M. (1985). The intracellular distribution and function of the high mobility group chromosomal proteins. *Exp. Cell Res.* **156**, 295-310.
Elton, T. S. and Reeves, R. (1986). Purification and postsynthetic modifications of Friend erythroleukemic cell high mobility group protein HMG-I. *Anal. Biochem.* **157**, 53-62.
Emsley, P. and Cowtan, K. (2004). Coot: model-building tools for molecular graphics. *Acta Crystallogr. D Biol. Crystallogr.* **60**, 2126-2132.
Gardella, S., Andrei, C., Ferrera, D., Lotti, L. V., Torrisi, M. R., Bianchi, M. E. and Rubartelli, A. (2002). The nuclear protein HMGB1 is secreted by monocytes via a non-classical, vesicle-mediated secretory pathway. *EMBO Rep.* **3**, 995-1001.
Gavel, Y. and von Heijne, G. (1990). Sequence differences between glycosylated and non-glycosylated Asn-X-Thr/Ser acceptor sites: implications for protein engineering. *Protein Eng.* **3**, 433-442.
Hao, P., Ren, Y. and Xie, Y. (2010). An improved protocol for N-glycosylation analysis of gel-separated sialylated glycoproteins by MALDI-TOF/TOF. *PLoS ONE* **5**, e15096.
Hebert, D. N., Lamriben, L., Powers, E. T. and Kelly, J. W. (2014). The intrinsic and extrinsic effects of N-linked glycans on glycoproteostasis. *Nat. Chem. Biol.* **10**, 902-910.
Hoppe, G., Talcott, K. E., Bhattacharya, S. K., Crabb, J. W. and Sears, J. E. (2006). Molecular basis for the redox control of nuclear transport of the structural chromatin protein Hmgb1. *Exp. Cell Res.* **312**, 3526-3538.
Hori, O., Brett, J., Slattery, T., Cao, R., Zhang, J., Chen, J. X., Nagashima, M., Lundh, E. R., Vijay, S., Nitecki, D. et al. (1995). The receptor for advanced glycation end products (RAGE) is a cellular binding site for amphoterin: mediation of neurite outgrowth and co-expression of rage and amphoterin in the developing nervous system. *J. Biol. Chem.* **270**, 25752-25761.
Ito, I., Fukazawa, J. and Yoshida, M. (2007). Post-translational methylation of high mobility group box 1 (HMGB1) causes its cytoplasmic localization in neutrophils. *J. Biol. Chem.* **282**, 16336-16344.
Kimura, K., Katoh, N., Sakurada, K. and Kubo, S. (1985). Phosphorylation of high mobility group 1 protein by phospholipid-sensitive Ca2+-dependent protein kinase from pig testis. *Biochem. J.* **227**, 271-276.
Kwak, M. S., Lim, M., Lee, Y. J., Lee, H. S., Kim, Y. H., Youn, J. H., Choi, J. E. and Shin, J.-S. (2015). HMGB1 binds to lipoteichoic acid and enhances TNF-α and IL-6 production through HMGB1-mediated transfer of lipoteichoic acid to CD14 and TLR2. *J. Innate immun.* **7**, 405-416.
Leahy, D. J., Rule, G. S., Whittaker, M. M. and McConnell, H. M. (1988). Sequences of 12 monoclonal anti-dinitrophenyl spin-label antibodies for NMR studies. *Proc. Natl. Acad. Sci. USA* **85**, 3661-3665.
Li, J., Wang, H., Mason, J. M., Levine, J., Yu, M., Ulloa, L., Czura, C. J., Tracey, K. J. and Yang, H. (2004). Recombinant HMGB1 with cytokine-stimulating activity. *J. Immunol. Methods* **289**, 211-223.
Lotze, M. T. and Tracey, K. J. (2005). High-mobility group box 1 protein (HMGB1): nuclear weapon in the immune arsenal. *Nat. Rev. Immunol.* **5**, 331-342.
Lu, B., Nakamura, T., Inouye, K., Li, J., Tang, Y., Lundbäck, P., Valdes-Ferrer, S. I., Olofsson, P. S., Kalb, T., Roth, J. et al. (2012). Novel role of PKR in inflammasome activation and HMGB1 release. *Nature* **488**, 670-674.
Marshall, R. D. (1974). The nature and metabolism of the carbohydrate-peptide linkages of glycoproteins. *Biochem. Soc. Symp.*, **40**, 17-26.
Min, H. J., Ko, E. A., Wu, J., Kim, E. S., Kwon, M. K., Kwak, M. S., Choi, J. E., Lee, J. E. and Shin, J.-S. (2013). Chaperone-like activity of high-mobility group box 1 protein and its role in reducing the formation of polyglutamine aggregates. *J. Immunol.* **190**, 1797-1806.
Molinari, M. (2007). N-glycan structure dictates extension of protein folding or onset of disposal. *Nat. Chem. Biol.* **3**, 313-320.
Nyström, S., Antoine, D. J., Lundbäck, P., Lock, J. G., Nita, A. F., Högstrand, K., Grandien, A., Erlandsson-Harris, H., Andersson, U. and Applequist, S. E. (2013). TLR activation regulates damage-associated molecular pattern isoforms released during pyroptosis. *EMBO J.* **32**, 86-99.
Ombrellino, M., Wang, H., Ajemian, M. S., Talhouk, A., Scher, L. A., Friedman, S. G. and Tracey, K. J. (1999). Increased serum concentrations of high-mobility-group protein 1 in haemorrhagic shock. *Lancet* **354**, 1446-1447.
Park, J. S., Svetkauskaite, D., He, Q., Kim, J.-Y., Strassheim, D., Ishizaka, A. and Abraham, E. (2004). Involvement of toll-like receptors 2 and 4 in cellular activation by high mobility group box 1 protein. *J. Biol. Chem.* **279**, 7370-7377.
Reeves, R. and Chang, D. (1983). Investigations of the possible functions for glycosylation in the high mobility group proteins. Evidence for a role in nuclear matrix association. *J. Biol. Chem.* **258**, 679-687.
Reeves, R., Chang, D. and Chung, S. C. (1981). Carbohydrate modifications of the high mobility group proteins. *Proc. Natl. Acad. Sci. USA* **78**, 6704-6708.
Salmivirta, M., Rauvala, H., Elenius, K. and Jalkanen, M. (1992). Neurite growth-promoting protein (amphoterin, p30) binds syndecan. *Exp. Cell Res.* **200**, 444-451.
Scaffidi, P., Misteli, T. and Bianchi, M. E. (2002). Release of chromatin protein HMGB1 by necrotic cells triggers inflammation. *Nature* **418**, 191-195.
Schiraldi, M., Raucci, A., Munoz, L. M., Livoti, E., Celona, B., Venereau, E., Apuzzo, T., De Marchis, F., Pedotti, M., Bachi, A. et al. (2012). HMGB1 promotes recruitment of inflammatory cells to damaged tissues by forming a complex with CXCL12 and signaling via CXCR4. *J. Exp. Med.* **209**, 551-563.
Schwarz, F. and Aebi, M. (2011). Mechanisms and principles of N-linked protein glycosylation. *Curr. Opin. Struct. Biol.* **21**, 576-582.
Sha, Y., Zmijewski, J., Xu, Z. and Abraham, E. (2008). HMGB1 develops enhanced proinflammatory activity by binding to cytokines. *J. Immunol.* **180**, 2531-2537.
Sterner, R., Vidali, G. and Allfrey, V. G. (1979). Studies of acetylation and deacetylation in high mobility group proteins. Identification of the sites of acetylation in HMG-1. *J. Biol. Chem.* **254**, 11577-11583.
Stott, K., Tang, G. S., Lee, K.-B. and Thomas, J. O. (2006). Structure of a complex of tandem HMG boxes and DNA. *J. Mol. Biol.* **360**, 90-104.
Sun, I. Y., Johnson, E. M. and Allfrey, V. G. (1980). Affinity purification of newly phosphorylated protein molecules. Thiophosphorylation and recovery of histones H1, H2B, and H3 and the high mobility group protein HMG-1 using adenosine 5′-O-(3-thiotriphosphate) and cyclic AMP-dependent protein kinase. *J. Biol. Chem.* **255**, 742-747.
Sundén-Cullberg, J., Norrby-Teglund, A., Rouhiainen, A., Rauvala, H., Herman, G., Tracey, K. J., Lee, M. L., Andersson, J., Tokics, L. and Treutiger, C. J. (2005). Persistent elevation of high mobility group box-1 protein (HMGB1) in patients with severe sepsis and septic shock. *Crit. Care Med.* **33**, 564-573.
Tang, D., Kang, R., Livesey, K. M., Cheh, C.-W., Farkas, A., Loughran, P., Hoppe, G., Bianchi, M. E., Tracey, K. J., Zeh, H. J.III et al. (2010). Endogenous HMGB1 regulates autophagy. *J. Cell Biol.* **190**, 881-892.
Tanuma, S.-I., Yagi, T. and Johnson, G. S. (1985). Endogenous ADP ribosylation of high mobility group proteins 1 and 2 and histone H1 following DNA damage in intact cells. *Arch. Biochem. Biophys.* **237**, 38-42.
Thorburn, J., Horita, H., Redzic, J., Hansen, K., Frankel, A. E. and Thorburn, A. (2009). Autophagy regulates selective HMGB1 release in tumor cells that are destined to die. *Cell Death Differ.* **16**, 175-183.
Tian, J., Avalos, A. M., Mao, S.-Y., Chen, B., Senthil, K., Wu, H., Parroche, P., Drabic, S., Golenbock, D., Sirois, C. et al. (2007). Toll-like receptor 9–dependent activation by DNA-containing immune complexes is mediated by HMGB1 and RAGE. *Nat. Immunol.* **8**, 487-496.
Valliere-Douglass, J. F., Eakin, C. M., Wallace, A., Ketchem, R. R., Wang, W., Treuheit, M. J. and Balland, A. (2010). Glutamine-linked and non-consensus asparagine-linked oligosaccharides present in human recombinant antibodies define novel protein glycosylation motifs. *J. Biol. Chem.* **285**, 16012-16022.
Wang, H., Bloom, O., Zhang, M., Vishnubhakat, J. M., Ombrellino, M., Che, J., Frazier, A., Yang, H., Ivanova, S., Borovikova, L. et al. (1999). HMG-1 as a late mediator of endotoxin lethality in mice. *Science* **285**, 248-251.
Watson, M., Stott, K. and Thomas, J. O. (2007). Mapping intramolecular interactions between domains in HMGB1 using a tail-truncation approach. *J. Mol. Biol.* **374**, 1286-1297.
Welply, J. K., Shenbagamurthi, P., Lennarz, W. J. and Naider, F. (1983). Substrate recognition by oligosaccharyltransferase. Studies on glycosylation of modified Asn-X-Thr/Ser tripeptides. *J. Biol. Chem.* **258**, 11856-11863.
Yang, H., Hreggvidsdottir, H. S., Palmblad, K., Wang, H., Ochani, M., Li, J., Lu, B., Chavan, S., Rosas-Ballina, M., Al-Abed, Y. et al. (2010). A critical cysteine is required for HMGB1 binding to Toll-like receptor 4 and activation of macrophage cytokine release. *Proc. Natl. Acad. Sci. USA* **107**, 11942-11947.
Yang, L., Xie, M., Yang, M., Yu, Y., Zhu, S., Hou, W., Kang, R., Lotze, M. T., Billiar, T. R., Wang, H. et al. (2014). PKM2 regulates the Warburg effect and promotes HMGB1 release in sepsis. *Nat. Commun.* **5**, 4436.
Yang, H., Wang, H., Ju, Z., Ragab, A. A., Lundback, P., Long, W., Valdes-Ferrer, S. I., He, M., Pribis, J. P., Li, J. et al. (2015). MD-2 is required for disulfide HMGB1-dependent TLR4 signaling. *J. Exp. Med.* **212**, 5-14.
Youn, J. H. and Shin, J.-S. (2006). Nucleocytoplasmic shuttling of HMGB1 Is regulated by phosphorylation that redirects it toward secretion. *J. Immunol.* **177**, 7889-7897.
Youn, J. H., Oh, Y. J., Kim, E. S., Choi, J. E. and Shin, J.-S. (2008). High mobility group box 1 protein binding to lipopolysaccharide facilitates transfer of lipopolysaccharide to CD14 and enhances lipopolysaccharide-mediated TNF-α production in human monocytes. *J. Immunol.* **180**, 5067-5074.
Zou, J., Kawai, T., Tsuchida, T., Kozaki, T., Tanaka, H., Shin, K.-S., Kumar, H. and Akira, S. (2013). Poly IC triggers a cathepsin D- and IPS-1-dependent pathway to enhance cytokine production and mediate dendritic cell necroptosis. *Immunity* **38**, 717-728.

Journal of Cell Science